Large, Deployable S-Band Antenna for a 6U Cubesat

Peter A. Warren, John W. Steinbeck, Robert J. Minelli
Physical Sciences, Inc.
20 New England Business Center Andover, MA 01810; 978-689-0003
pwarren@psicorp.com

Carl Mueller
Vencore, Inc.
1100 Apollo Drive Brook Park, OH 44142; 216-977-0090
carl.mueller@vencore.com

ABSTRACT

Small satellites in general and cubesats in particular have been limited in their ability to perform RF science and communications missions by the size of the RF aperture. A large deployable membrane antenna approach has been developed to address the limits in aperture size and provide both high gain communications and sensing from UHF to C-band. The paper describes the general approach and presents performance results from ground test articles of an S-Band implementation of the architecture. The test article deploys a 1.53 m^2 active area out of a 2U (2,000 cm^3) volume from a 6U cubesat. The antenna array is formed from two tensioned membranes. The membranes are folded compactly for launch along with four deployable boom structures. Once on orbit, the booms deploy, unfolding and tensioning the membranes and then hold them in place for operation. Ground test articles have shown a gain of 30.5 dB at 3.6 GHz. The antenna has a 3 dB beamwidth of 3.4°, has an overall aperture efficiency of 56% and sidelobes 10 dB lower than the main lobe. The system architecture can be applied to payload volumes as small as ½U and to frequencies from UHF to K-band.

INTRODUCTION

Small spacecraft are very appealing for many missions because of their reduced cost and ease of access to space via ride-share or other low cost launch opportunities. However, several classes of small satellite are limited in their mission by the size of the RF aperture with which to communicate or perform passive and active remote sensing.

Cubesat[1] missions, in particular, are limited by the small size both of the spacecraft and of the exposed surfaces available for antenna mounting. For this reason, many developers have deployed cubesat antennas[2] from simple dipoles[2,4], to helixes[4], to parabolic dishes[6]. These systems have been effective in their mission performance, but are still limited in their aperture and gain.

MECHANICAL PERFORMANCE

Overall architecture

In order to provide a large an aperture as possible out of the limited cubesat volume, the authors used membranes that are plated with a conductor and then selectively etched to provide both an array of patch antennas and the feed network that drives that array. As can be seen in Figure 1, the antenna array is laid out on a Cartesian grid, requiring a rectangular active area.

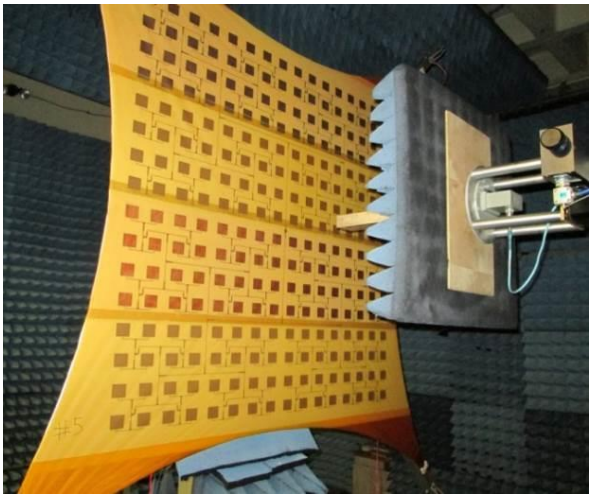

Figure 1: 3.6 GHz Membrane Antenna Prototype in Near-Field RF Test Range

The membranes are tensioned at the corners by a deployable structure that provides the load required to flatten the membranes, maintain their relative separation, and to point them accurately.

Stowed Configuration

The membranes stow by flattening the space between the broadcast plane and the ground plane and then folding

the two layers simultaneously. The structure stows independently underneath the stowed antenna. Many configurations are possible, but in the implementation discussed in this paper, the antenna payload is stowed in 2U at one end of a 6U cubesat (Figure 2).

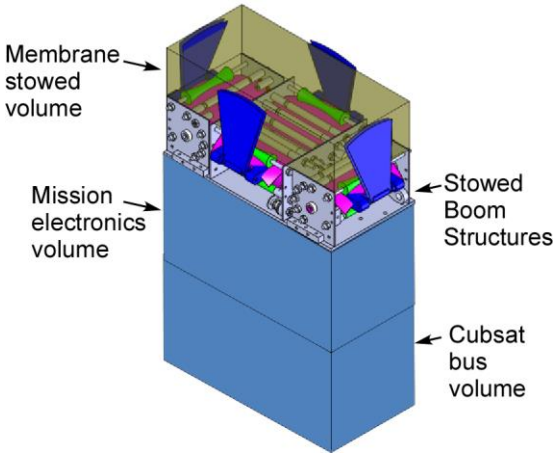

Figure 2: Layout of system in stowed configuration

As shown in Figure 2, the stowed deployable boom structures and their drive mechanisms fit in a 2U footprint and are 7 cm thick. The stowed membranes are 1.3 cm thick, leaving 1.7 cm as room for growth with larger apertures than that tested. The membranes have a mass of 336 gm and the four booms themselves have a mass of 109 gm. The remainder of the 1.5 kg weight allocation is made up of the restraint, drive, and mounting hardware.

The system architecture allows the membrane antenna portion and the deployable structure portions to be treated as modular elements. They are integrated separately, reducing risk and easing testing. The modularity also allows the same deployable structure to be used for a broad range of wavelengths and dimensions without requiring reconfiguration, redesign, or requalification.

Deployment of the booms and membranes

The system is constrained for launch by a sprung, hinged lid held closed by a burn wire. Upon command, the lid opens and flips out of the way with the membrane constrained by the tensioning arrangement at the ends of the booms.

The booms then deploy away from the spacecraft either all four simultaneously or in sequence as opposing pairs. Deploying all four booms at once requires less drive and control hardware, but results in higher overall membrane deployment drag. Sequential deployment provides more control in the deployment and reduces the overall membrane creasing.

Figure 3 shows the deployment steps of the antenna membranes when all four booms are deployed simultaneously. The cables shown in the figure were to gather deployment load data. This load data is shown in Figure 4.

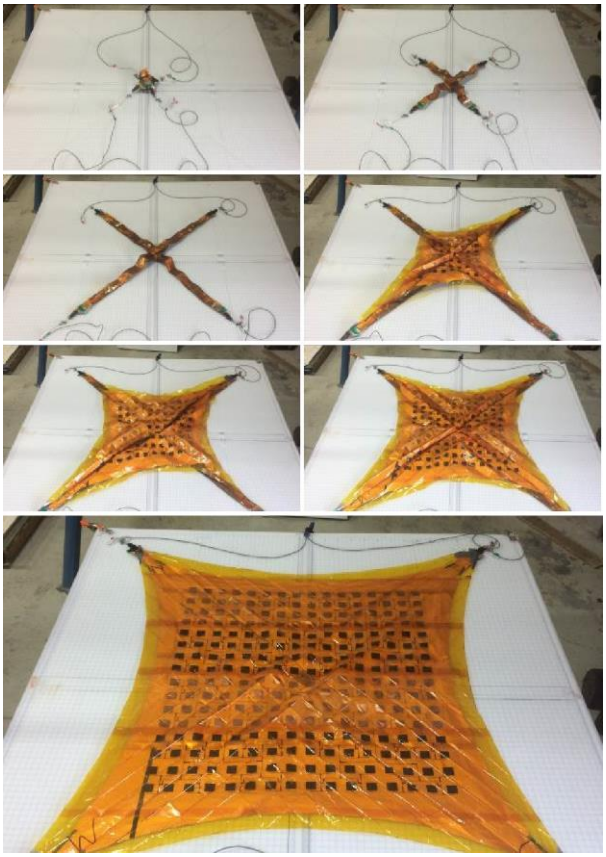

Figure 3: Simultaneous deployment steps of a 16x16 element antenna

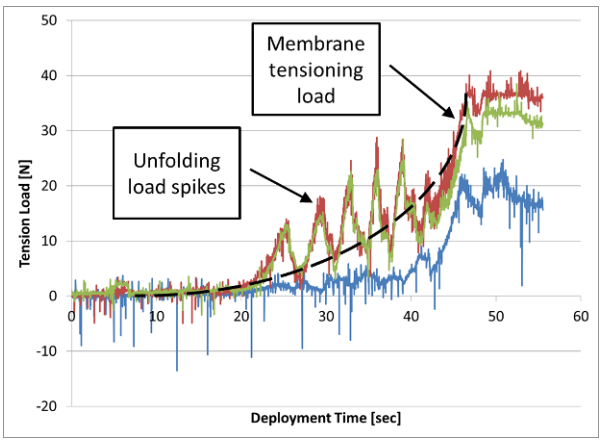

Figure 4: Deployment drag over the course of the simultaneous deployment of the 16x16 element antenna

As can be seen in Figure 4, the initial stages of the deployment have very little drag with levels below the noise floor of the load cell (1-3 N). During the final stages of the deployment, the membrane tension begins to ramp up (dotted line). As the larger folds in the membrane unfurl and pull through fold inversions, there are periodic load spikes and subsequent relaxations.

The deployable booms are derived from the well-characterized Storable Tube Extensible Member (STEM)[7]. Each boom is designed to support a total load of 220N. The maximum tension needed to pull the antenna membranes flat for operation is 100 N. The maximum drag seen in the deployment trials was 40N. Consequently, the system has more than adequate structural margin for both deployment and tensioning.

An alternate means of deploying the membranes is to deploy a pair of opposing booms first and then deploy the second pair. This deployment sequence is shown in Figure 5.

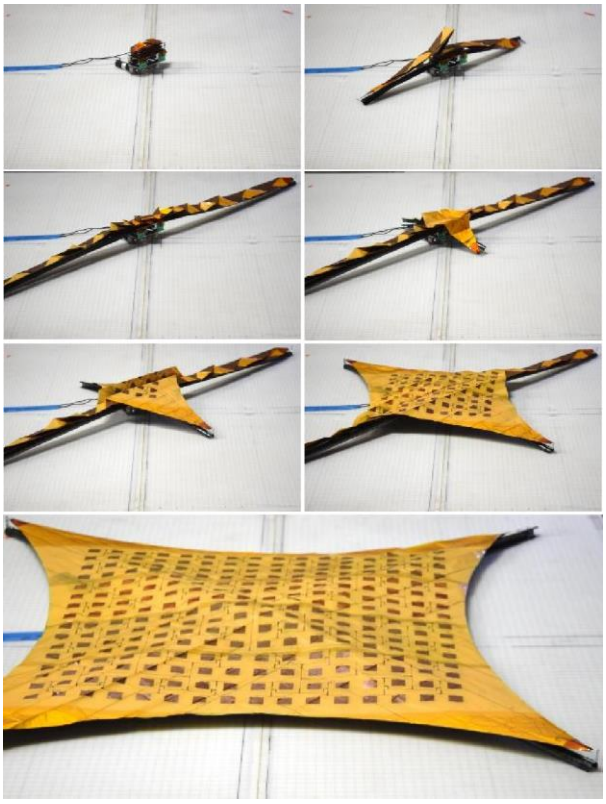

Figure 5: Sequential deployment of 16x16 element antenna

RF PERFORMANCE

Non-creased performance

As shown in Figure 1, the antenna was mounted vertically and tested in a planar near field range. For all test configurations, a 4λ distance (36.4 cm at 3300 MHz) is maintained between the antenna and rectangular waveguide probe. For all test cases the phased array antenna is the transmit antenna, and the waveguide probe is the receive antenna. The test is conducted by scanning the waveguide probe over a planar surface (scan plane), and measuring the signal amplitude and phase (S parameter, S21) at slightly less than λ/2 increments in the vertical and horizontal directions. Figure 6 shows a two-dimensional map of the far-field radiation pattern at elevation and azimuth angles from 0° to ± 60°. It is calculated by applying a Fourier transform to signal amplitude and phase measurements taken at the scan plane. It's noteworthy that the main lob is well defined, with 3 dB beamwidths = 3.3 – 3.5°, which is close to the design goals of 3.4°.

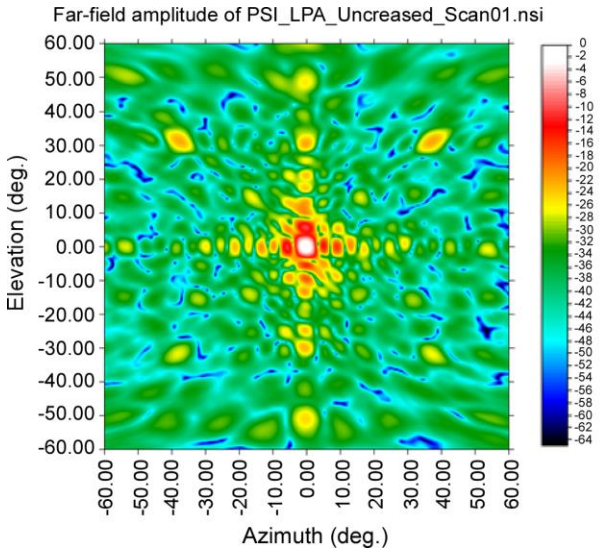

Figure 6: Two-dimensional plot of far-field radiation pattern (3600 MHz). 3 dB beamwidth = 3.3 – 3.5°

Figure 7 shows antenna gain (top) and antenna directivity and aperture efficiency (bottom) as a function of frequency from 3300 – 3900 MHz, at membrane tip loads ranging from 20 – 67 N. The variation in tip load was provided to understand the effects of tension on the RF performance.

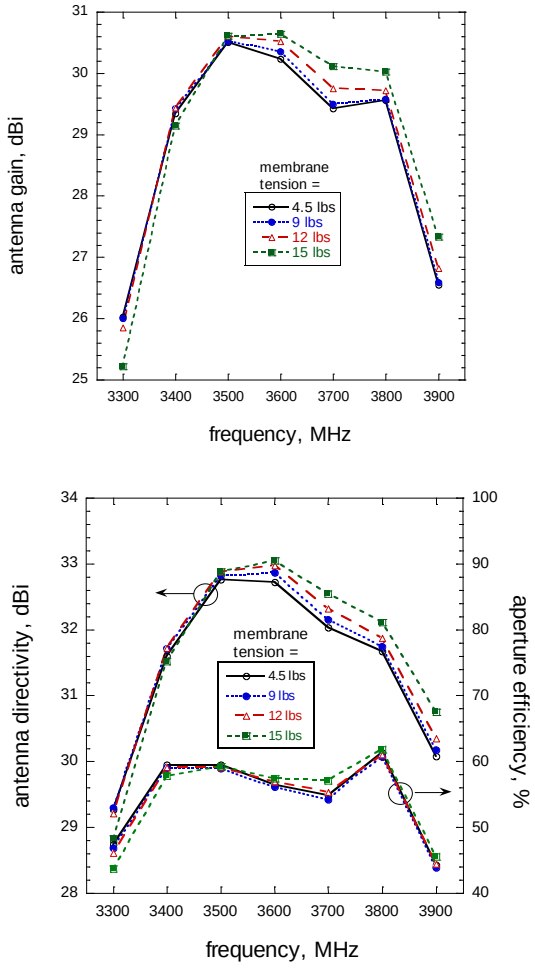

Figure 7: Antenna gain (top) and antenna directivity and aperture efficiency (bottom) as a function of frequency from 3300 – 3900 MHz

The antenna is designed for optimal gain at 3600 MHz, although the performance is almost as good at 3500 MHz. Below 3500 MHz there is no significant difference in antenna performance at different tension levels. Above 3500 MHz the antenna gain improves with increasing tension levels. From 3400 – 3800 MHz, the aperture efficiency ranges from 55 – 60%. Figure 8 shows that at 3600 MHz and 12 lbs. (53N) tension, the antenna gain is 30.5 dBi and aperture efficiency = 56%. The highest sidelobe is approximately 10 dB lower than the main lobe, and cross-polarization levels are better than 20 dB below the co-polarization peak. The H-plane cross-polarization levels are approximately 10 – 15 dB higher than the E-plane cross polarization levels, which indicates a higher tendency for co-polarized power radiated in the E-plane to couple to the H-plane, as opposed co-polarized H-plane/cross-polarized E-plane coupling.

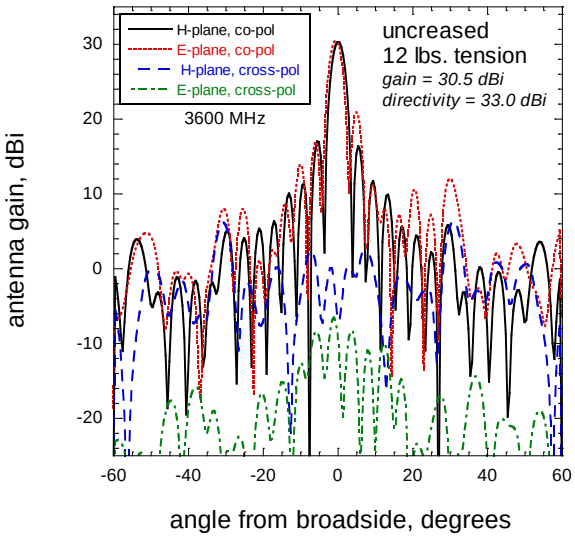

Figure 8: Two-dimensional Co- and cross-polarization antenna patterns in the electric field (E-plane) and magnetic field planes (H-plane)

Aperture images in Figure 9 and Figure 10 show that the antenna aperture is well-defined, but there are discernable variations in amplitude and phase across the aperture. The amplitude varies over ~ 10 dB range; while the phase is reasonably constant over large areas, there are some locations where the phase varies by up to 180° over small areas. It is likely that degradation from ideal antenna performance is directly tied to phase variations across the aperture, which in turn leads to amplitude variation and somewhat degraded antenna gain and aperture efficiency. The variations do not appear to have a systematic pattern.

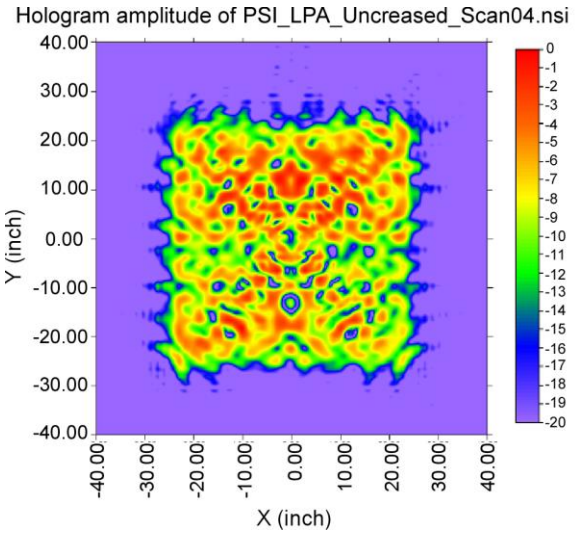

Figure 9: Amplitude hologram at antenna aperture

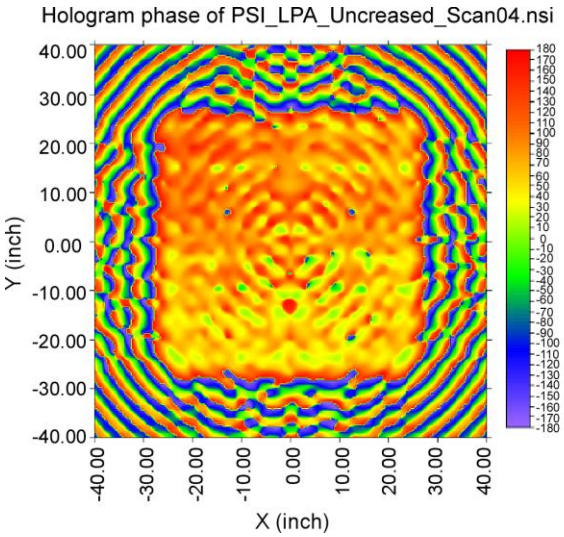

Figure 10: Phase hologram at antenna aperture

The as-modeled antenna performance was 32.7 dBi. The phase variations across the aperture shown in the figures above result in a 2 dB reduction in overall performance and thus will be the subject of future design refinement.

Effects of folding

One of the clear concerns of this antenna architecture is the effects of folding and deployment on the RF performance of the membranes. The ductile nature of the copper conductor that forms the antenna means that folding the antenna will create creases along with the wrinkles and ripples that result from imperfect handling and tensioning. These imperfections change the local capacitance between the broadcast layer and ground plane and can introduce phase errors and partial internal reflections.

The authors folded the antenna shown in Figure 1 three times using a repeatable set of tooling and compressing the antenna thoroughly each time before unfolding and tensioning it. Once the antenna has been folded, the creases are visually apparent. Even with high tension levels, the wrinkles cannot be fully removed.

The folding pattern used was the more aggressive simultaneous deployment pattern. Additionally, the antenna was folded so that it would fit in a ½U volume. These two folding choices resulted in a crease pattern that was both deeper and more spatially frequent to provide a conservative indication of the impacts of membrane folding. Figure 11 shows a rear view of the ground plane after repeated folding, illustrating the folding pattern. Figure 12 shows the front side of the same antenna, but under higher tension load. Again, the folding crease pattern can be clearly seen.

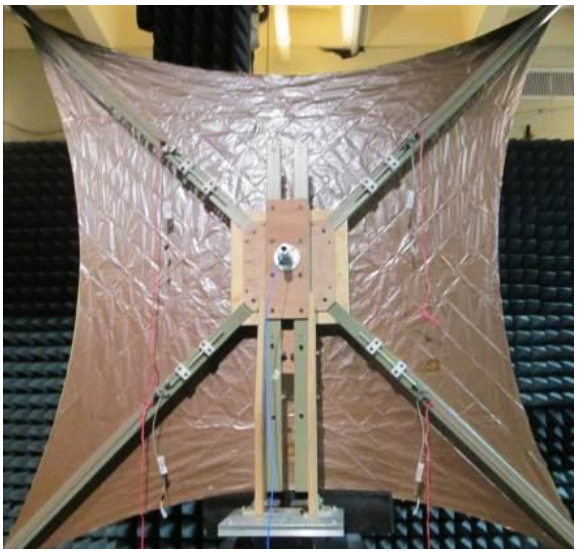

Figure 11: The back side of the ground plane after repeated folding and deployment at 18N tip load

Figure 12: The front side of the broadcast plane after repeated folding and deployment at 110N tip load

After being folded and deployed three times, the membranes were tensioned with a 110N tip load and the antenna performance was measured. Figure 13 plots co- and cross-polarization radiation patterns in the E- and H-planes, at 3600 MHz and 25 lbs. tension, for the antenna folded three times. The antenna gain is 28.7 dBi and aperture efficiency = 50%. The highest sidelobe is ~ 10 dB lower than the main lobe, and the H-plane

cross-polarization levels are comparable, and better than 25 dB below the co-polarized main lobe levels.

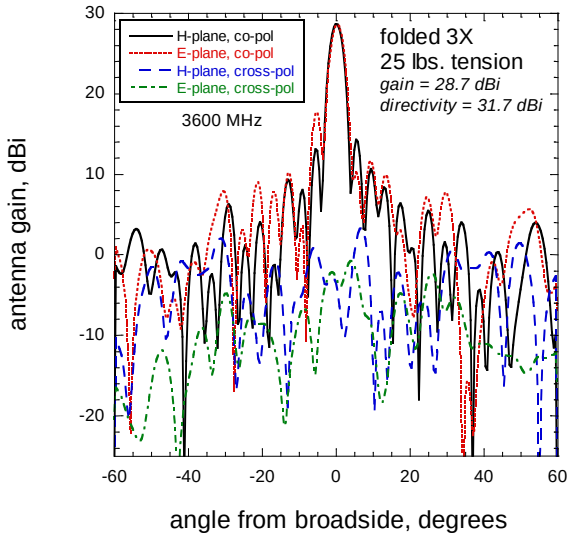

Figure 13: Membrane antenna performance after being folded 3 three times. 110 N tip load.

This performance is a 1.9 dBi reduction from the as-measured performance of a non-folded antenna. Figure 14 and Figure 15 show the holograms for amplitude and phase respectively. As can be seen in the figures, both the amplitude and phase show zones of reduced contribution to the overall antenna performance. This is attributed to regions of local phase delays and reflections from the antenna creases.

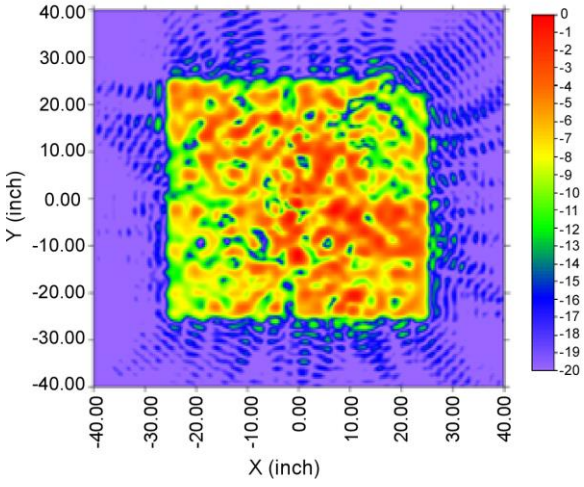

Figure 14: Amplitude hologram at antenna aperture after three fold/deploy cycles and 110N tension

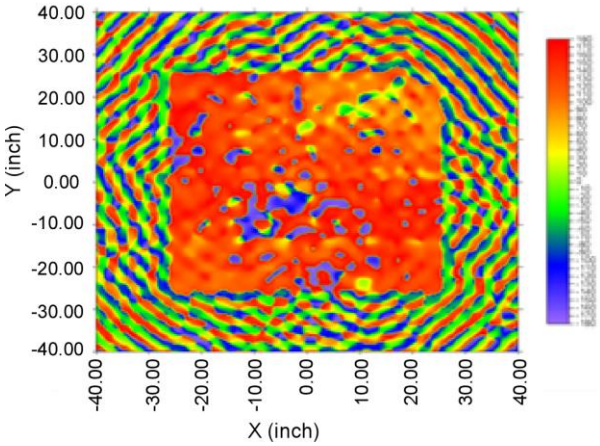

Figure 15: Phase hologram at antenna aperture after three fold/deploy cycles and 110N tension

After observing the crease patterns that result from the folding, the authors believe it possible to design a folding pattern that will reduce the crease amplitude and depth. Similarly, the diagnostic holograms shown above will be combined with other data to reduce the phase errors at the individual elements to provide a more uniform and efficient aperture.

As shown in Table 1, even with the reduced gain from the creasing, the 1.3m on a side antenna provided performance of a perfect parabola 1.0m in diameter without the complexity of a deployed feed. As the phase distribution issues are addressed through design and the crease issues addressed through mechanical alterations to the membrane, the system performance has the potential to reach the equivalent performance of a 1.5m rigid dish.

Table 1: Summary of antenna performance and equivalent idealized parabolic dish

Case	Gain	Equivalent Rigid Parabolic Dish
Idealized antenna, no losses	34 dBi	1.9 m
As modelled with inherent material losses	32.7 dBi	1.5m
As tested with no creases	30.5 dBi	1.2m
As tested after three fold-deploy cycles and tensioned	28.6 dBi	1.0m

Other configurations and future work

In addition to the 1.73 m^2, 3.6 GHz antenna discussed in detail above, the authors have built and tested a variety of other membrane antennas with the same overall architecture. Antennas of various sizes have been built and tested at 912 MHz, as well as at 1.2, 1.85[8], 3.6, 6.5, and 8.0 GHz. Deployable configurations have been designed for as small as ½U payloads and for

as large as ESPA-class satellites[8]. In general, smaller antennas are more efficient with some providing efficiencies of 85-90%. This dependence on feed line path length implies that there are effects that are not as yet captured by the design tools and would be a productive area of future work.

SUMMARY AND CONCLUSIONS

A corporate-fed strip antenna was constructed using two thin membranes with appropriately designed conductive patterns. The membranes were folded compactly along with a four-boom deployable structure into a 2U payload volume for a 6U cubesat. Testing has shown that the deployment drag of the membranes from their folded state is well within the load margins of the deployable boom designs. RF testing has shown that the antenna provides 30.5 dBi of gain at 3.6 GHz when un-creased and 28.6 dBi of gain when folded and deployed several times and then tensioned to an appropriate level.

Acknowledgments

This material is based upon work supported by the United States Air Force under Contract No. FA9453-14-C-0034. In addition, the authors would like to acknowledge the technical support of Dr. Jeremy Banik of Air Force Research Laboratory, Space Vehicles Directorate.

References

1. Heidt, H., J. Puig-Sauri, A. Moore, S. Nakasuka, and R. Twiggs, "CubeSat: A new generation of Picosatellite for education and industry low-cost space experimentation," in Proc. 14th Annual AIAA/USU Conference on Small Satellite, Logan, UT, Aug. 2000
2. Frost, C. Agasid, E. et al "Small Spacecraft Technology State of the Art," NASA TP-2014-216648, Ames Research Center, Moffett Field, CA, January 2014
3. Costantine, J., Y. Tawk, C.G. Christodoulou, J. Banik, S. Lane, "CubeSat Deployable Antenna Using Bistable Composite Tape-Springs," Antennas and Wireless Propagation Letters, IEEE Volume: 11
4. Murphey, T.W., S. Jeon, A. Biskner, and G. Sanford, "Deployable booms and antennas using Bi-stable tape-springs," in Proc. 24th AIAA/USU Conference on Small Satellites, Logan, UT, 2010
5. Costantine, J., Y. Tawk, A. Ernest, C.G. Christodoulou, "Deployable antennas for CubeSat and space communications," Antennas and Propagation (EUCAP), 2012 6th European Conference on Publication Year: 2012
6. MacGillivray, C.S., "Miniature Deployable High Gain Antenna for CubeSats," 2011 CubeSat Developers Workshop April 20 - 22, 2011
7. Rimrott, F.P.J., "Storable tubular extendable members," Engineering Digest, September 1966.
8. Mueller, C.H., P.A. Warren, J.W. Steinbeck, "High-Gain, L-Band Membrane Phased Array Antenna for Small Satellites," IEEE Transactions on Antennas and Propagation, in submittal.